IMAGE GRADIENT BASED SHAPE PRIOR FOR THE SEGMENTATION OF NOT THAT SPHERICAL STRUCTURES

Sebastian Steger and Georgios Sakas

Fraunhofer Institute for Computer Graphics Research IGD, Darmstadt, Germany

ABSTRACT

A popular method for the segmentation of somewhat spherical structures (e.g. certain types of tumors, lymph nodes, lung nodules) from 3D medical images is sending out radial rays from a central point and determining the most likely radius for each ray, resulting in a closed surface. Besides satisfying some image based criteria, a regularization term or shape prior typically ensures a smooth contour by preferring similar radii of neighboring rays.

In this paper we show that the structures it is often applied to, are in fact not that spherical. We propose an alternate shape prior depending on the gradient direction, preferring smooth structures that are not necessarily spherical.

We quantitatively evaluate the proposed shape prior with the traditionally used shape prior on a set of 49 lymph nodes from clinical images. A dice similarity coefficient improvement of 4% has been observed (0.80 vs. 0.77), yielding in segmentation accuracy close to manual segmentation (DSC of 0.83).

***Index Terms*—** Segmentation, Radial Rays, Spherical Structures, Lymph Node, Shape Prior

1. INTRODUCTION

Segmentation of various structures from medical images is required for analysis, therapy planning and visualization. Due to low contrast, low resolution, noise and other modality specific imaging artifacts, automated segmentation of structures from medical images is particularly challenging. Well known purely image based standard segmentation techniques such as region growing typically fail when applied to medical images. Instead background knowledge about the size, shape and texture needs to be incorporated in the segmentation process.

A popular approach is the adaption of a model to image data (e.g. [1]). This has the great advantage that low contrast object boundaries can nevertheless be found based on the model knowledge, just as a human would intuitively do. The less instances of the same object class differ from each other in terms of size, shape and texture, the better model based approaches work in general.

In reverse, structures with large variety cannot be segmented equally well because fewer a priori assumptions can be made, and thus the risk of boundary leaking and the adaption to wrong entities is increased. Besides that, the typically only local optimal model adaptations result in a high sensitivity towards the model's initial position and size, thereby increasing the risk of adaption to wrong entities even further.

The well known snakes algorithm [2] and its countless variants master the just described challenge by using local instead of global shape priors. For somewhat spherical objects another popular approach to do so, is to send out radial rays from a given seed point within the object and then determine the most probable radius for all rays jointly. The result is a closed path/surface around the seed point in 2D/3D respectively. In 2D, this has for example been done for the segmentation of lesions in mammography [3] and lymph nodes [4]. In 3D, this approach has been applied to lymph nodes [5] [6], gliomas [7] and interactive segmentation of tumors [8]. Note that for these segmentation algorithms the supported set of object shapes is theoretically bound to the star domain, as each point on the surface requires a straight connection to the seed point.

A local shape prior typically ensures that the radii of neighboring rays shall be as similar as possible, enforcing a smooth surface. The underlying assumptions are that the shape of the object is close to a sphere and the seed point is close to the center. The less the assumption can be applied, the smaller the contribution of local shape prior has to be, while still being able to obtain a segmentation of the target object. In return this increases the risk of leaking into wrong structures.

In many cases this assumption indeed is not very applicable. For example healthy lymph nodes typically have the shape of a bean (see background of Fig. 2). Also, tumors are known for their unpredictable shape, highly depending on the surrounding tissue.

In this work, we present a local shape prior that is based on the image gradient, intending to cover a wider range of structures being not that spherical. This shape prior is then compared to the state of the art shape prior in a radial ray based segmentation algorithm. Belief propagation is used for energy minimization. Quantitative evaluation is done on representative set of 49 lymph nodes in CT images for which ground truth segmentation is available.

This work is partially funded within the NeoMark project (FP7-ICT-2007-2-224483) by the European Commission.

2. SEGMENTATION OF SPHERICAL STRUCTURES

A user defined seed point is given. From that point n rays are casted in all possible directions so that they are uniformly distributed on a surrounding circle/sphere (see Fig. 1). The task of the segmentation algorithm is to assign a single radius r_i to each ray i, thereby considering image information (data term) as well as knowledge about the shape (e.g. smoothness). This results in a closed contour/surface around the seed point. This data structure is naturally suited for spherical objects, but can also be used for all convex structures and some star convex structures.
Typically an energy of the following form is assigned to each possible configuration $\boldsymbol{r}$:

$$E(\boldsymbol{r}) = \sum_{\forall i} cd_i(r_i) + \sum_{j \in N(i)} cs_i(r_i, r_j) \;, \qquad (1)$$

where $N(i)$ are all neighboring rays of ray i, cd_i is its data depending cost at a specific radius r_i and cs_i is its shape depending cost for the transition of the radius r_i to the radius r_j of the neighboring ray j. Thus the segmentation process essentially becomes a minimization problem.

2.1. Data Terms

The data term assigns a cost cd to each radius of each ray in order to guide the segmentation algorithm. The data term depends on the input image and is typically tailored to a very specific field of application using a heuristic. [8] is based on the image gradient, [4] combines this with expected intensities in the interior and [7] uses gray value differences. and [6] is based on intensity homogeneity and its variation. [5] uses the distance to the most likely radius which was determined based on image intensities, and [3] uses a combination of known gray level distribution, edge based information and a size prior.

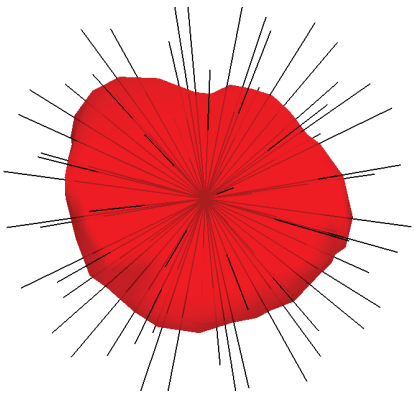


Fig. 1. Radial rays and closed surface around seed point.

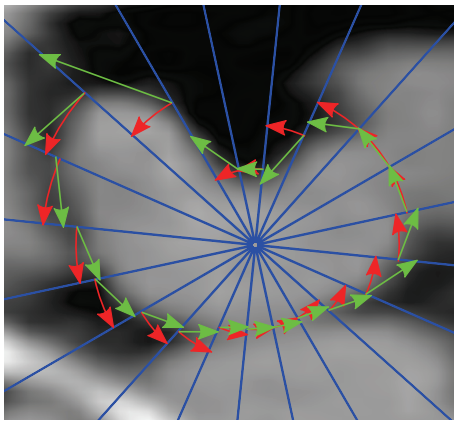


Fig. 2. Zero cost transition of the sphere shape prior (red) and the proposed image gradient based shape prior (green) on the boundary of a typical lymph node.

2.2. Shape Priors

All of the previously mentioned radial ray based segmentation methods have one thing in common: Its shape cost is minimal if the target structure is a sphere with the seed point in its center. While the graph based methods [7] and [6] achieve this because of their graph creation strategy, all others ensure that the radii of neighboring rays r_i and r_j are as similar as possible. A popular (used in [5], [4] and [8]) and easy to implement way to do so, is to deploy a shape prior of the form

$$cs_i(r_i, r_j) = \lambda |r_i - r_j|^\gamma \;, \qquad (2)$$

where r_i and r_j are radii of two neighboring rays, γ controls the stiffness and λ the impact relative to the data term. From now on, we will refer to it as the *sphere shape prior* because of its preference for spherical structures.
However, the shapes this kind of shape prior is used on in practice, are in many cases not spherical enough to achieve satisfactory segmentation results (see red contours in Fig. 4(a),4(b)). Especially when then angle between a ray and the object's boundary is small, assuming that a neighboring ray will have a similar radius is not a good idea as illustrated by the red arrows in Fig. 2.

2.3. Optimization

The final segmentation path/surface is obtained by minimizing the energy functional given by (1). In 2D, dynamic programming based algorithms find the optimal path efficiently [4][3]. However, in the 3D case no efficient optimal algorithm is known. Thus local or global optimization techniques are deployed, such as gradient decent in [5], graph cut in [7][6] and belief propagation in [8]. Global optimization techniques have the advantage that no initial values are required which is especially desirable if the objects have a large variance in size.

Metric	Gradient based shape prior			Shere shape prior			Manual Segmentation		
	min	max	avg	min	max	avg	min	max	avg
Dice Similarity Coefficient	0.50	0.94	0.80 ± 0.10	0.52	0.91	0.77 ± 0.11	0.24	0.94	0.83
Volume Overlap Error	11.15	66.33	32.41 ± 13.17	15.87	65.31	36.32 ± 14.00	10.54	86.11	27.65
Average Surface Distance	0.15	2.15	0.61 ± 0.42	0.14	2.21	0.74 ± 0.47	0.14	2.75	0.42
Maximum Surface Distance	1.20	13.45	4.60 ± 3.08	1.08	16.61	4.53 ± 2.96	1.00	18.18	3.18

Table 1. Comparison between the proposed gradient based shape prior and sphere shape prior on 49 lymph nodes from CTs.

3. IMAGE GRADIENT BASED SHAPE PRIOR

In the previous section we have seen that all mentioned ray based segmentation algorithms prefer the shape of a sphere despite the fact that the structures they are used on may actually be not that spherical. Instead, we propose to use a shape prior that is based on the direction of the image gradient. Equation (2) is extended to

$$cs_i(r_i, r_j) = \lambda |g_{i,j}(r_i) - r_j|^\gamma \,, \tag{3}$$

where

$$g_{i,j}(r_i) = \begin{cases} r_i & \text{if } ||\nabla I(r_i \boldsymbol{a_i})|| < \text{grad}_{\text{min}} \\ \frac{\nabla I(r_i \boldsymbol{a_i}) \cdot \boldsymbol{a_i}}{\nabla I(r_i \boldsymbol{a_i}) \cdot \boldsymbol{a_j}} r_i & \text{otherwise} \end{cases} \tag{4}$$

is the intersection of ray i (direction unit vector $\boldsymbol{a_i}$)'s neighboring ray j (direction $\boldsymbol{a_j}$) and the plane defined by the point $r_i \boldsymbol{a_i}$ and the normal direction given by the image gradient $\nabla I(r_i \boldsymbol{a_i})$ (see Fig. 4). Since small gradients (i.e. smaller than some threshold grad_{min}) possibly result from noise and thus are not meaningful, the sphere shape prior is used in those cases.

Incorporating the direction of the image gradient the proposed shape prior does not prefer spheres, but shapes actually present in the image. Looking at the green arrows in Fig. 2, the target structure – in this case the lymph node – is clearly preferred by the proposed shape prior.

4. EXPERIMENTS & RESULTS

The segmentation performance of the proposed gradient based shape prior has been compared to the sphere shape prior on 49 lymph nodes. Both shape priors were used in the same ray based segmentation framework described in the previous sections. The data term depends on the intensities in the interior as well as on the image gradient (for details see [4]). Belief propagation is used for the optimization of (1). In order to evaluate only the impact of the different shape priors on the segmentation performance, the manually selected seed points and all parameters have been set identically, except the shape prior's weight λ, which was determined using an exhaustive search on the test set.

The validation set consists of 49 lymph nodes from clinically acquired CT images. It contains benign as well as malign lymph nodes, their 3D long to short axis ratio (aspect ratio) ranging from 1.2 up to 2.7. Whereas the shape of some of them was pretty close to a sphere, others were really not that spherical. Ground truth was obtained by the STAPLE [9] algorithm applied to manual segmentations of 5 different radiologists.

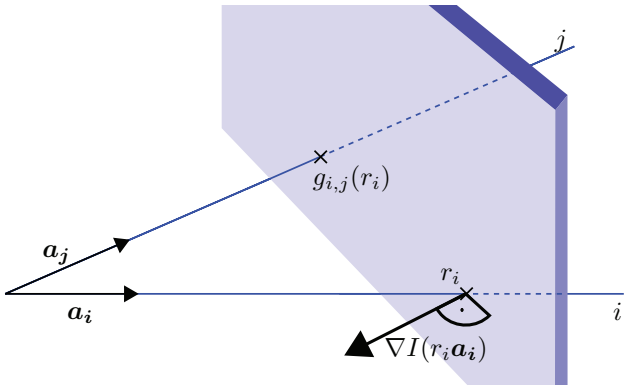
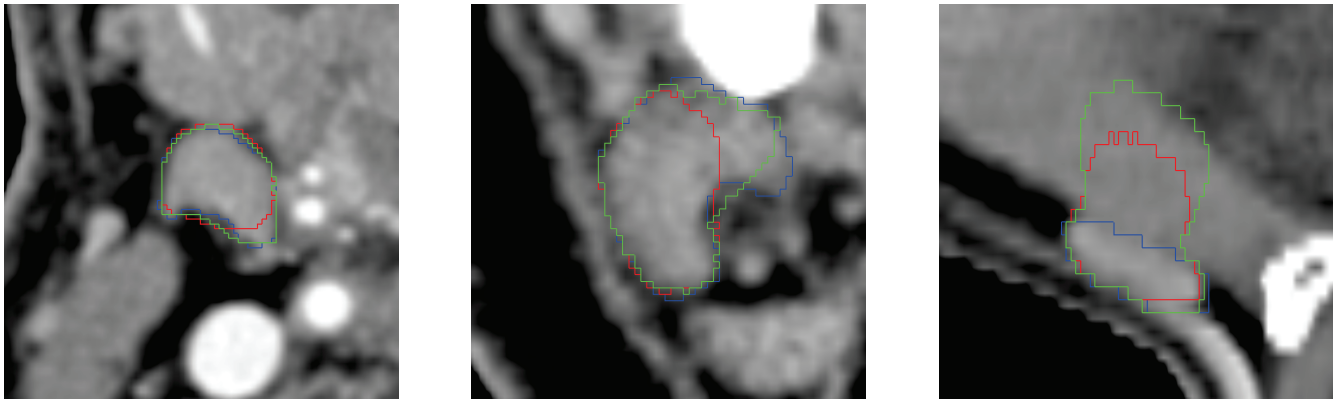


Fig. 3. Plane through r_i intersects neighboring ray. Normal vector is given by image gradient direction.

The same segmentation algorithm with the two different shape priors was run on that validation set and the results were compared to ground truth using the *dice similarity coefficient* (DSC), *volume overlap error* (VOE), *average surface distance* (ASD) and *maximum surface distance* (MSD). It turned out that using the proposed image gradient based shape prior resulted on the average in a 4% increase in terms of DSC (0.80 vs. 0.77) with a slightly lower standard deviation for the proposed shape prior. For comparison, the manual segmentations of the radiologists achieved an average DSC of 0.83. See Fig. 4 for some examples and table 1 for all results.

In a second experiment we tried to assess the performance improvement in relation to the deviation from the spherical shape. As a quantitative measure for that shape deviation we simply used the aspect ratio of minimum volume enclosing box. For different aspect ratios the performance gain can be seen in Fig. 5. Despite some outliers due to low image contrast at the actual object boundary (see Fig. 4(c)), a higher average improvement was achieved for larger aspect ratios. This confirms our design goal to cope better with not that spherical objects.



(a) Improvement in the bottom right corner (b) Improvement on not spherical node (c) Failure due to low contrast

Fig. 4. Sample segmentation results (ground truth in blue, proposed shape prior in green and sphere shape prior in red)

5. CONCLUSION

This paper presented a novel shape prior to be used in a radial ray based segmentation scheme. The traditional shape prior prefers spherical structures despite the fact that many of the structures the technique has been used on (e.g. lymph nodes, tumors) are in fact not that spherical. In contrast to that the proposed shape prior prefers structures that are actually persisting in the image by tracing the structure orthogonal to the image gradient direction.

It has been compared to the traditional sphere shape prior on a representative set of 49 lymph nodes for which ground truth segmentation is available. With an average DSC of 0.80 the proposed shape prior results in a DSC gain of 4% compared to the sphere shape prior and is close to manual segmentation. As expected, segmenting objects with a larger aspect ratio, i.e. not that spherical, result in a higher performance gain.

6. REFERENCES

[1] T. Heimann and H.P. Meinzer, "Statistical shape models for 3d medical image segmentation: A review," *Medical Image Analysis*, vol. 13, no. 4, pp. 543–563, 2009.

[2] M. Kass and et al., "Snakes: Active contour models," *International Journal of Computer Vision*, vol. 1, pp. 321–331, 1988.

[3] S. Timp et al., "A new 2d segmentation method based on dynamic programming applied to computer aided detection in mammography.," *Med Phys*, vol. 31, no. 5, pp. 958–971, 2004.

[4] S. Steger et al., "Lymph node segmentation in ct slices using dynamic programming," in *IEEE International Symposium on Biomedical Imaging*, 2011, pp. 1990–93.

[5] A. Barbu et al., "Automatic detection and segmentation of axillary lymph nodes," in *MICCAI 2010*, vol. 6361 of *LNCS*, pp. 28–36. Springer, 2010.

[6] Y. Wang wt al., "Graph-based segmentation of lymph nodes in ct data," in *Advances in Visual Computing*, vol. 6454 of *LNCS*, pp. 312–321. Springer, 2010.

[7] Jan Egger et al., "Nugget-cut: A segmentation scheme for spherically- and elliptically-shaped 3d objects," in *Pattern Recognition*, vol. 6376 of *LNCS*, pp. 373–382. Springer, 2010.

[8] S. Steger et al., "Fist: Fast interactive segmentation of tumors," in *MICCAI Workshop on Computational and Clinical Applications in Abdominal Imaging*, 2011.

[9] S. K. Warfield, K. H. Zou, and W. M. Wells, "Simultaneous truth and performance level estimation (staple): an algorithm for the validation of image segmentation," vol. 23, no. 7, pp. 903–921.

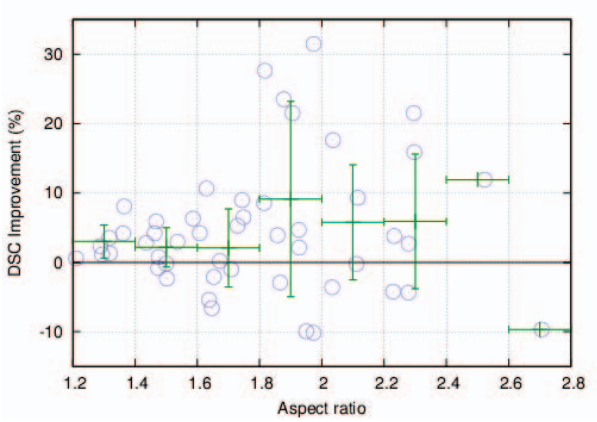


Fig. 5. DSC improvement of the presented shape prior with respect to the aspect ratio of the lymph node.